

Production of platelets *in vitro* in functionalized 3-dimensional scaffolds mimicking the bone marrow niche

Holly R. Foster,^{1*} Maria Colzani,^{1*} Guenaelle Bouet,^{1*} Daniel Howard,^{1*} Christian A. Di Buduo,²⁺ Nicole Müller-Sienerth,³ Amie K. Waller,¹ Yi Sun,⁴ Natalia Davidenko,⁴ Jennifer H. Shepherd,⁴ Thomas Moreau,¹ Amanda L. Evans,¹ Paolo M. Soprano,² Martin E. M. Parsons,^{5,6} Yumi Ying Sims,⁷ Meera Arumugam,¹ Wardiya Afshar-Saber,¹ Ernest Turro,⁸ Patricia B. Maguire,^{5,6} Serena M. Best,⁴ Ruth E. Cameron,⁴ Alessandra Balduini,^{2,9} Gavin J. Wright^{3,10} and Cedric Ghevaert¹

¹Wellcome-MRC Cambridge Stem Cell Institute, Jeffrey Cheah Biomedical Center, Cambridge Biomedical Campus, University of Cambridge, Cambridge, UK; ²Department of Molecular Medicine, University of Pavia, Pavia, Italy; ³Cell Surface Signaling Laboratory, Wellcome Trust Sanger Institute, Cambridge, UK; ⁴Department of Materials Science and Metallurgy, Cambridge Center for Medical Materials, University of Cambridge, Cambridge, UK; ⁵SPHERE Research Group, UCD Conway Institute, University College Dublin, Dublin, Ireland; ⁶School of Biomolecular and Biomedical Science, University College Dublin, Dublin, Ireland; ⁷Wellcome Trust Sanger Institute, Cambridge, UK; ⁸Department of Genetics and Genomic Sciences, Icahn School of Medicine at Mount Sinai, New York, NY, USA; ⁹Department of Biomedical Engineering, Tufts University, Medford, MA, USA and ¹⁰Department of Biology, Hull York Medical School, York Biomedical Research Institute, University of York, York, UK

*HRF, MC and GB contributed equally as first authors.

+DH and CADB contributed equally.

Correspondence: C. Ghevaert
cg348@cam.ac.uk

A. Balduini
alessandra.balduini@unipv.it

Received: October 9, 2024.

Accepted: April 17, 2025.

Early view: April 24, 2025.

<https://doi.org/10.3324/haematol.2024.286758>

©2025 Ferrata Storti Foundation
Published under a CC BY license



Abstract

The safety, quality and supply of donor-derived platelet units intended for transfusion have improved over the past decades but significant problems still remain. *In vitro*-derived platelets offer a possible alternative but up-scaling production is hindered by our limited understanding of thrombopoiesis (the release of platelets by their mother cell, the megakaryocyte [MK]). Here, we have developed an integrated strategy aiming to mimic *ex vivo* the bone marrow physiological niche that promotes thrombopoiesis by mature MK. The screening of a panel of 259 recombinant transmembrane proteins derived from cells known to promote platelet production through direct contact with MK enabled us to show that ACVR1B, CRTAM, MUCEN and BTN1A1 improve platelet production from either cord blood- (ACVR1B) or pluripotent stem cells-derived (CRTAM, MUCEN and BTN1A1) MK. Using two different methodologies, we functionalize either collagen- or silk-based 3-dimensional scaffolds and confirm increased functional platelet production by up to 2-fold. This unbiased approach has allowed us to identify novel proteins whose role in platelet formation was previously unknown and highlights the potential gain of recreating the MK niche to allow *in vitro* platelets to become a viable alternative for transfusion.

Introduction

Platelets are small anucleate blood cells produced by megakaryocytes (MK) in the bone marrow. Their primary function is to promote coagulation and blood vessel repair at sites of injury. In the UK, NHS Blood and Transplant has seen a 20% increase in platelet demand over the past decade with 280,000 platelet units being distributed per year.¹

We are solely reliant on donors to source platelets which in itself, presents several issues. Short shelf lives (5-7 days, as opposed to 35 days for red blood cells), HLA typing, allogenic platelet transfusions and risks of viral/bacteria transmission all add strain to a fragile supply chain. We believe that *in vitro* production of platelets could offer a viable alternative to donor-dependent platelets for transfusion and could address these issues. MK derived from renewable stem cell

sources such as human pluripotent stem cells have already been well documented with high MK yields and purity.²⁻⁴ They offer an on-demand supply of platelets with control over immune-compatibility and biosafety.⁵ Unfortunately, the numbers of platelets *in vitro* MK can produce are several orders of magnitude less than the estimated 1,000-2,000 platelets per MK produced *in vivo*. Even with bioreactor systems that allow us to mimic bone marrow architecture and mechanical stresses such as shear flow and turbulence, numbers are still very low; 1 to 100 per MK platelets depending on the type of bioreactor system that was used and, particularly, depending on the stringency of the criteria used to characterize the “platelet output”.⁶⁻¹² Physical stresses, although essential, are not enough to recreate *in vivo* thrombopoiesis and therefore there must be other factors involved.^{7,13,14}

Several groups have highlighted the importance of MK-endothelial cell interactions in the regulation of platelet production¹⁵⁻¹⁸ as well as other cell types such as mesenchymal stem cells.¹⁹ However, these studies have not focused on identifying the proteins and signaling pathways involved in cross-talk between MK and supportive cells. In addition, positive MK-to-MK feed-back loops have also been described that promote platelet formation.^{20,21} Here we analyze proteomic profiles of several cell types or cell lines (including MK) that promote platelet production by cultured MK *in vitro* in order to identify cell surface and/or secreted proteins that can be used to functionalize bioreactor systems to recreate the chemical, as well as physical bone marrow niche and thereby enhance platelet production.

Methods

Cell culture

Cord blood-derived megakaryocytes

CD34⁺ cells were isolated from cord blood obtained with full consent in accordance with Cambridgeshire 4 Research Ethics Committee (07/MRE05/44), the Ethical Committee of the I.R.C.C.S. Policlinico San Matteo Foundation of Pavia, and the principles of the Declaration of Helsinki. Cord blood (CB) samples were obtained according to institutional guidelines upon informed consent of the parents. Cord blood-derived megakaryocytes (CBMK) were cultured using previously described protocols.² Alternative protocols were used for silk experiments.²² Only cultures that were above 70% CD41a/CD42a double-positive and above 90% DAPI-negative were deemed mature, viable CBMK and used in further experiments.

Induced pluripotent stem cell-derived megakaryocytes

Induced pluripotent stem cell (iPSC) line ‘A1ATD1’, was obtained from Cambridge Biomedical Research Center iPSC Core Facility MK and was differentiated into MK using previously published protocols.²¹⁴ For iPSC-MK, cultures were used in further experiments if above 70% CD41a/CD42a double-positive and above 30% DAPI-negative.

Feeders

C3H/10T1/2 (gift from Prof Koji Eto, CIRA, Japan) were cultured in Basal Medium Eagle medium supplemented with 10% fetal bovine serum (FBS). OP9 cells were cultured in GlutaMax α -MEM supplemented with 20% FBS. Mouse embryonic fibroblasts (MEF) were cultured using Advanced DMEM/F12 supplemented with 10% FBS and 2 mM L-glutamine. MSC (gift from Dr John Girdlestone, NHSBT) and were cultured using Advanced DMEM/F12 supplemented with 10% FBS and 2 mM L-glutamine. Human umbilical vein endothelial cells (HUVEC) and human brain microvascular endothelial cells (HBMEC) were cultured using Endothelial Cell Basal Medium-2 supplemented with EGM SingleQuots (Lonza). HBMEC and MEF were cultured on 0.01% gelatin- (Sigma) coated wells.

Platelet production assay

For co-culture

For HBMEC and MEF, wells were coated with 0.01% gelatin for 2 hours (h) at room temperature (r.t.). Feeders were seeded at 7×10^4 cells/mL in their indicated media and incubated overnight at 37°C in a 5% CO₂ humidified incubator.

MK were centrifuged at 100 g for 5 minutes at r.t. and resuspended to 5×10^5 – 1×10^6 cells/mL (2D/3D) in Cellgro only. Wells were washed with Cellgro only. Semi-dehydrated scaffolds were transferred to a 96-well plate. Cells were seeded (100 μ L/well) and incubated for 24/72 h at 37°C (iPSC-MK/CB-MK respectively). Flow cytometry analysis was performed using a previously published protocol and gating strategy indicated in *Online Supplementary Figure S1*.⁶ Platelets were quantified during flow cytometry analysis using Flow-Count Fluorospheres (Beckman Coulter, gated on in *Online Supplementary Figure S1*).

Proplatelet formation assay

In multi-well plates: proplatelet assays were performed using previously published protocols using Maxisorp 96-well plates.²³ For silk films: silk films were lifted off the PDMS, trimmed using a biopsy punch, and secured to the bottom of a 24-well plate using silicon rings. Before cell seeding, silk films were soaked in cell culture media for 1 h. Cells were centrifuged 100 g/120 g (CBMK/iPSC-MK) and resuspended in StemSpan; 50,000 cells were seeded per silk film and incubated for at least 16 h at 37°C. Cells were fixed with 4% paraformaldehyde (Sigma Aldrich) for 20 minutes at r.t. Samples were processed using a previously published protocol and probed with anti- β 1-tubulin (1/1,000, Abcam) and Alexa secondary antibody (1/500, ThermoFisher Scientific).²⁴

Production of 3-dimensional collagen scaffolds and functionalization with recombinant transmembrane proteins

Porous collagen cell supports were formed following a previously published protocol using 0.05 M acetic acid.²⁵ Porous collagen was crosslinked at a 5/2/1 ratio of 1-ethyl-3-(3-dimethylaminopropyl)carbodiimide, hydrochloride/

N-hydroxysuccinimide/carboxylate groups in the protein (EDAC/NHS/COO-) present in the collagen molecules with EDAC in 70% volume/volume ethanol.²⁶ At the crosslinking stage, a biotin side chain was added by including an amine-polyethylene glycol 2 (PEG2)-Biotin (EZ-Link, Thermo Scientific) at 300 µg/mg collagen. Crosslinking was performed for 3 h before being washed three times 70% ethanol and left for 48 h in 70% ethanol before rinsing in excess DPBS and base media overnight before use.

Production of 3-dimensional silk scaffolds and functionalization with recombinant transmembrane proteins

Silk solution (8% weight/volume) was mixed with 10 or 20 µg/mL of recombinant transmembrane proteins (recTMP) alone or in combination and cast into a molding chamber.²⁴ NaCl particles (approximately 500 µm in diameter) were then sifted into the solution in a ratio of 1 mL to 2 g of NaCl particles. The scaffolds were then placed at r.t. for 48 h and finally soaked in distilled water for 48 h to leach out the salt. Before cell seeding, silk scaffolds were sterilised and soaked in cell culture media for 1 h.

Bioreactor set-up

The 3D silk scaffolds were set up using a previously published protocol.²⁴ The perfusion of the silk scaffold was performed at 80 µL/min.

Collected platelets produced *ex vivo* were analyzed by flow cytometry using the same forward and side scatter pattern as human peripheral blood and identified as CD41⁺CD42b⁺ events. Isotype controls were used as a negative control to exclude non-specific background signal. Platelet number was calculated using a TruCount bead standard. All samples were acquired with a Beckman Coulter Navios flow cytometer and analyzed using Beckman Coulter Navios software package.

For the analysis of platelet spreading, 25 µg/mL type I collagen was coated onto glass coverslips at 4°C, overnight. *Ex vivo*-produced platelets were allowed to adhere for 60 minutes at 37°C. Samples were probed and analyzed using a previously published protocol.²⁷

Results

A library of recombinant receptor ectodomains to create a niche that promotes platelet formation

Several cell types have been previously shown to promote platelet production from MK in co-culture systems, these include murine cell lines (OP9, C3H10T1/2), human endothelial cells and macrophages.²⁸⁻³⁶ We first sought to confirm these results by culturing MK in a co-culture with different cell lines chosen on the hypothesis that they would either support platelet formation or be a neutral control.³⁷ We observed a small trend towards an increase in platelet

production with C3H/10T1/2, (1.92-fold change \pm 0.81 standard deviation [SD]; $P=0.085$) and a significant increase with both endothelial cell types; HUVEC (1.90-fold change \pm 0.60 SD; $P<0.05$) and HBMEC (1.73-fold change \pm 0.41 SD; $P<0.05$; *Online Supplementary Figure S2A*) compared to the non-feeder control. OP9 and the negative control cell type had no significant effect compared to the non-feeder control. Conditioned media from these cell lines had no effect on platelet production, confirming the necessity for direct cell-to-cell contact to promote platelet production (*Online Supplementary Figure S2B*).

We postulated therefore that protein expressed on the surface of the supportive cells or potentially secreted protein through a localized paracrine effect may promote platelet formation. We generated proteomics data from cell lysates and performed transcriptome array analysis from each cell line. Candidate proteins found in the proteome/transcriptome of cells supportive of platelet formation were shortlisted on the basis that they contained a putative signal peptide and transmembrane region, indicating a potential localization to the membrane. We then compared data from supportive cell lines with cell lines that did not promote platelet formation in co-cultures. From the comparison between C3H/10T1/2 (which promoted platelet formation) and OP9 and MEF (which did not), 25 candidates were shortlisted using the proteomics data and nine from the transcriptome analysis (*Online Supplementary Table S1*). Comparing human cell lines HUVEC and BMEC (which promoted platelet production) to MSC (which did not), 30 candidates were identified from the proteomics data and 125 from the transcriptome analysis, giving a total of 189 shortlisted proteins that are enriched in supportive cell lines compared to non-supportive (*Online Supplementary Table S2*).

Extensive libraries also exist of platelet surface membrane proteins and secretomes.²⁰ As positive feedback loops potentially exist between platelets and MK, we decided to also screen 97 candidate proteins expressed by human platelets identified through proteomics (*Online Supplementary Table S3*).^{20,21} A total of 286 proteins were therefore selected for the next step.

Identification of recombinant proteins that increase platelet production

We have previously shown how the entire ectodomains of membrane-embedded proteins can be expressed in a soluble recombinant form (recTMP) by the transient transfection of the human cell line, HEK293.³⁸ From our 286 shortlisted proteins, 259 were successfully expressed as recTMP, as confirmed by western blot (*Online Supplementary Tables S1-3*). These 259 recTMP were expressed, purified, quantified and immobilized on streptavidin-coated microtitre plates at a single concentration of 10 µg/mL. A rat Cd4 enzyme-linked immunosorbent assays (ELISA) was performed to confirm their immobilization onto the plates with an

optical density above that of wells containing streptavidin only (*Online Supplementary Tables S1-3*). To determine if any of these recTMP could alter platelet production, mature CBMK or iPSC-MK were seeded into streptavidin-coated 96-well plates, where wells had been functionalized with the immobilized recTMP (Figure 1A).² Cells were harvested after 72/24 h (CBMK/iPSC-MK, respectively) and the number of platelets were quantified using flow cytometry and the following gating strategy: size and granularity compared to peripheral blood platelets (FS/

SS), metabolic viability (using calcein-AM dye) and CD41a/CD42b expression (*Online Supplementary Figure S1*). The number of platelets obtained in each recTMP-coated well was compared to the control well coated with streptavidin only. Out of the 259 recTMP screened with CBMK, 37 induced statistically significant increase in platelet production with a meta-analysis (21 recTMP; $P<0.05$; 16 recTMP; $P<0.01$; Figure 1B; *Online Supplementary Table S4*). Thirty-four recTMP significantly reduced platelet production (15 recTMP; $P<0.05$; 19 recTMP; $P<0.01$). For the iPSC-MK, in total 24 recTMP

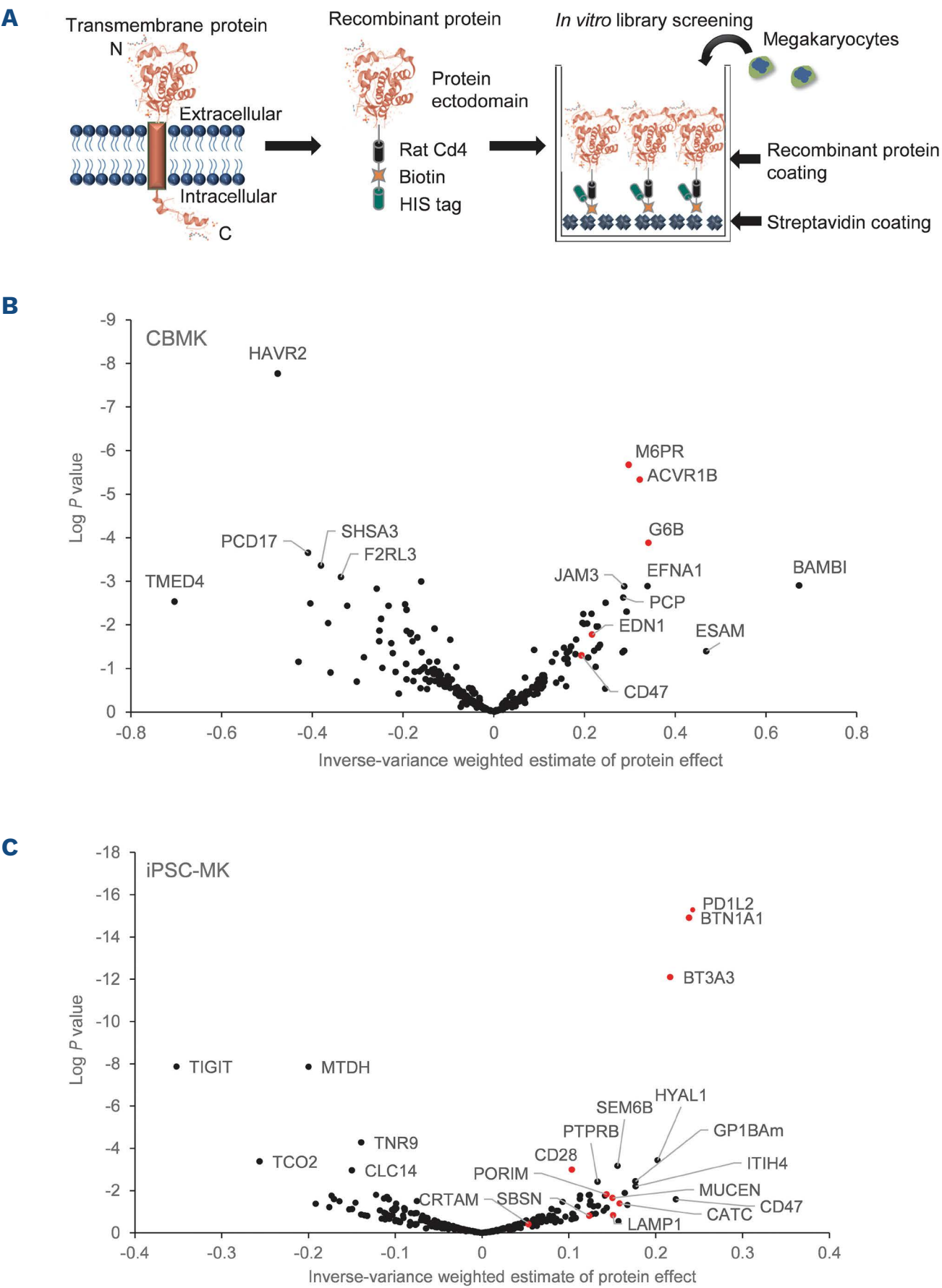


Figure 1. Recombinant transmembrane proteins can differentially affect platelet production. (A) Schematic representing how recombinant transmembrane proteins (recTMP) are produced from entire ectodomains of membrane-embedded proteins. These are tagged with rat Cd4 domain 3+4, biotin and 6-HIS tag, and immobilized on streptavidin-coated surfaces, megakaryocytes (MK) are cultured within these wells. Analysis of platelet production by flow cytometry of (B) cord blood-derived MK (CBMK) and (C) induced pluripotent stem cell derived-MK (iPSC-MK) incubated with individual recTMP at 10 $\mu\text{g}/\text{mL}$ for 72/24 hours (CBMK/iPSC-MK), data represents inverse-variance weighted estimate of protein effect versus log P value; $N=3-4$.

showed a statistically significant increase in platelet production with a meta-analysis (14 recTMP; $P < 0.05$; 10 recTMP; $P < 0.01$; Figure 1C; *Online Supplementary Table S5*). Fifteen recTMP significantly reduced platelet production (11 recTMP; $P < 0.05$; 5 recTMP; $P < 0.01$). Interestingly, only three recTMP, PD1L2 (#184), GP1Bam (#224) and PAR2 (110#) exhibited a significant positive effect on platelet production in both CBMK and iPSC-MK, although at a relatively low effect size in iPSC-MK. There was no cross-over of significantly negative recTMP.

To validate the results from the initial screen, a selection of positive proteins was chosen based on three selection criteria: (i) large relative size effect, (ii) low variance based on an adjusted P value less than 0.25 (*Online Supplementary Tables S4, S5*) and (iii) production efficiency (concentration). These candidate proteins (6 recTMP for CBMK and ten recTMP for iPSC-MK, highlighted as red dots in Figure 1B, C; *Online Supplementary Table S6*) had no overlap between the three datasets (mouse, human endothelium and platelet). All 16 proteins were analyzed again in the platelet production assay. Amongst the eight candidate CBMK recTMP; only ACVR1B was shown to significantly increase platelet production over the streptavidin control in these validation experiments (1.33 ± 0.22 fold change \pm SD; $P < 0.05$; Figure 2A; platelets/MK shown in *Online Supplementary Figure S3A*). Using the iPSC-MK recTMP; MUCEN, PD1L2, BTN1A1, BT3A3 and CRTAM significantly enhanced platelet production with a range of 1.29–1.39 relative fold change in this validation data set (Figure 2B; platelets/MK shown in *Online Supplementary Figure S3B*).

To confirm that our recTMP induced a true biological response, we first analyzed dose-response curves of four proteins that were validated above (selected based on highest effect and low variability) namely ACVR1B for CBMK and BTN1A1, CRTAM and MUCEN for iPSC-MK. These specific proteins were chosen based on the platelet production capabilities observed in both screens. Rat Cd4 ELISA confirmed the increased concentration of immobilized proteins amongst the range of concentrations tested (*Online Supplementary Figure S4A*). ACVR1B induced a dose-dependent, statistically significant, increase in platelet production, with the highest response obtained at the highest concentration tested ($40 \mu\text{g/mL}$) leading to a 2.03-fold change compared to the streptavidin only control (± 0.15 SD; $P < 0.001$; Figure 2C; platelets/MK shown in *Online Supplementary Figure S4B*). All three proteins tested with iPSC-MK exhibited a dose-dependent increase in platelet production too, albeit reaching a plateau with peak responses at $20 \mu\text{g/mL}$ (CRTAM), $10 \mu\text{g/mL}$ (BTN1A1) and $5 \mu\text{g/mL}$ (MUCEN, Figure 2D–F; expressed as platelets/MK in *Online Supplementary Figure 4C–E*). All three recTMP induced a similar maximal increase in platelet production at 1.49, 1.54, 1.77-fold change respectively (SD ± 0.23 , 0.22, 0.04, respectively).

We then decided to explore whether the gain in platelet production was driven by proplatelet formation (Figure 2G–

I). In CBMK, ACVR1B was shown to significantly increase the number of MK forming proplatelet extensions by $1.84 (\pm 0.86 \text{ SD})$; $P < 0.0001$; Figure 2H) whilst in the iPSC-MK, BTN1A1 and CRTAM both showed a significant increase in proplatelet formation (1.74 ± 0.25 and 2.05 ± 0.09 , respectively, fold change \pm SD; Figure 2I). Proplatelet formation was increased by MUCEN but it failed to reach significance ($P = 0.28$).

We then sought to investigate whether these recTMP exhibit additive or synergistic effects. Proteins were either combined in pairs or all three together in streptavidin-coated wells at the optimum concentration described above and platelet production was analyzed (*Online Supplementary Figure 5A–D*). No significant differences were observed between the combined proteins and their single counterparts. Quantification of recTMP per well using the rat Cd4 ELISA, revealed no increase in recTMP amount in the wells that were coated with two or three recTMP (*Online Supplementary Figure S5E, F*) compared to wells coated with the single protein at the optimal concentration identified from the dose-response curve. This indicates that the wells having combined recTMP were saturated and the concentration on the flat surface for each protein was likely below the concentration where we showed a maximum as a single protein.

Functionalizing materials for 3-dimensional scaffolds production

Two types of 3D scaffolds were selected for further work as they have been previously demonstrated to support platelet production *in vitro*, namely collagen- and silk-based scaffolds.^{6,24} These are low-shear, low-pressure systems that are able to be functionalized by the recTMP system.

Collagen scaffolds

The collagen scaffolds were functionalized using a biotin-streptavidin-biotin sandwich (Figure 3A). The biotinylated crosslinking was verified with streptavidin alkaline phosphatase attachment; it was possible to control the attachment of biotinylated side chains to the collagen cell supports by either limiting the amine-PEG-biotin linker concentration (“side chain limited”) or by reactant catalysis (EDAC/NHS) concentration and total amount (“x linker limited”; Figure 3B). Selecting the side chain limited method, streptavidin was added to the biotinylated scaffold and this was followed by the addition of the recTMP. The even distribution of the recTMP throughout the scaffold was checked with precipitation of insoluble BCIP/NBT (Figure 3C). Quantification of recTMP on the functionalized collagen scaffolds shows similar levels of recTMP in the single and the triple recTMP condition potentially indicating again a saturation point (Figure 3D). To validate whether the functionalized collagen scaffold could increase platelet production, we ran a platelet production assay under static conditions. With CBMK,

ACVR1B significantly increased platelet production by 2.47 ± 0.79 -fold compared to the streptavidin-only control (\pm SD; $P < 0.05$; Figure 3E; expressed as platelets/MK in *Online Supplementary Figure S6A*). For iPSC-MK, collagen scaffolds were functionalized using the recTMP CRTAM, BTN1A1 and MUCEN individually as well as all three combined using the same ratio of peak responses identified in the 2-dimensional experiments (4:2:1 CRTAM:BTN1A1:MUCEN). We did not see an increase in platelet production with BTN1A1 and MUCEN and there was a small increase with CRTAM (1.16 ± 0.13 fold change \pm SD; $P = 0.061$), however, when all three proteins were combined, we observed a statistically significant increase in platelet production over the streptavidin-only control (1.48 ± 0.16 , fold change \pm SD; $P < 0.05$; Figure 3F; expressed as platelets/MK in *Online Supplementary Figure S6B*).

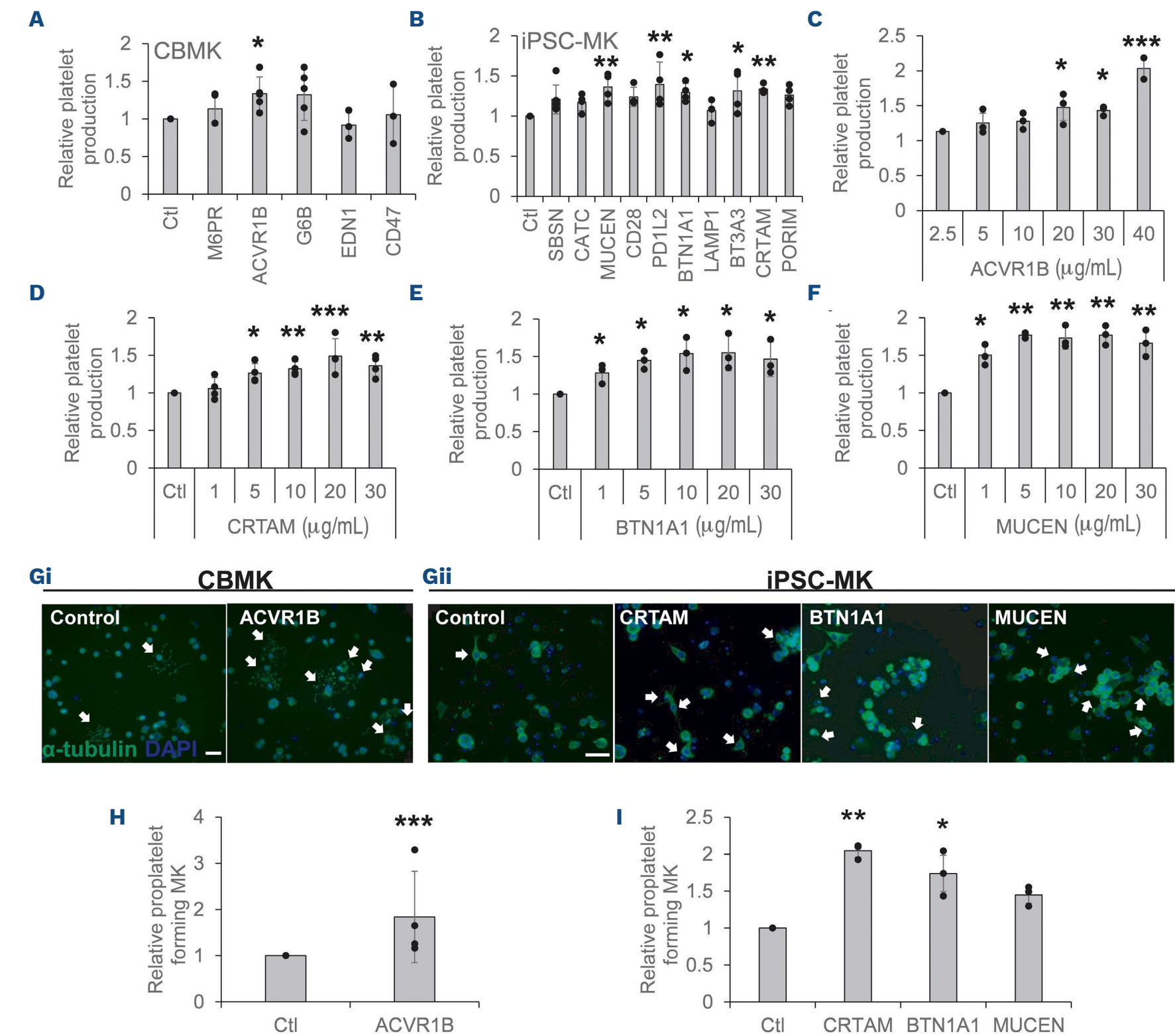


Figure 2. ACVR1B, MUCEN, BTN1A1 and CRTAM significantly increase platelet production and proplatelet formation. Analysis of platelet production by flow cytometry of (A) cord blood-derived megakaryocytes (CBMK), N=3-5, and (B) induced pluripotent stem cell-derived megakaryocytes (iPSC-MK), N=3-6, incubated with the indicated individual recombinant transmembrane proteins (recTMP) at 10 µg/mL for 72/24 hours (h) (CBMK/iPSC-MK). Analysis of platelet production by flow cytometry of (C), CBMK incubated for 72 h with the indicated concentrations of ACVR1B, N=3, and iPSC-MK incubated for 24 h with the indicated concentrations of (D) CRTAM, N=4, (E) BTN1A1, N=3 and (F) MUCEN, N=3. Analysis of proplatelet production on fibrinogen, representative images of (Gi) CBMK and (Gii) iPSC-MK incubated with the indicated individual recTMP at 10 µg/mL for 72/24 h (CBMK/iPSC-MK), DAPI (blue), α-tubulin (green), scale bar =20 µm. Quantification of proplatelet production of (H) CBMK, N=3, and (I) iPSC-MK, N=3, incubated with the indicated individual recTMP at 10 µg/mL for 72/24 h (CBMK/iPSC-MK). All data represents relative values compared to streptavidin-only control (Ctl). All data mean \pm standard deviation, repeated measures one-way ANOVA; * $P < 0.05$; ** $P < 0.01$; *** $P < 0.001$.

Silk films and scaffolds

Two types of silk scaffolds were used. First 2-dimensional films allowing the culture of cells at the top of the scaffold, followed by 3D silk sponges. To functionalize the silk films and 3D scaffolds, we adopted a strategy whereby we replaced the biotin tag of the recTMP described above with silk β -sheet binding sequence to allow the incorporation of

ACVR1B, CRTAM, BTN1A1 and MUCEN (*Online Supplementary Figure 7A*).³⁹ The BCIP/NBT analysis demonstrated efficient coating of the structure (*Online Supplementary Figure S7B*) and was further confirmed using an ELISA which showed the binding of alkaline phosphatase-conjugated antibodies at different concentrations of the peptides (10-20 $\mu\text{g}/\text{mL}$), with a very low signal in the negative controls (*Online*

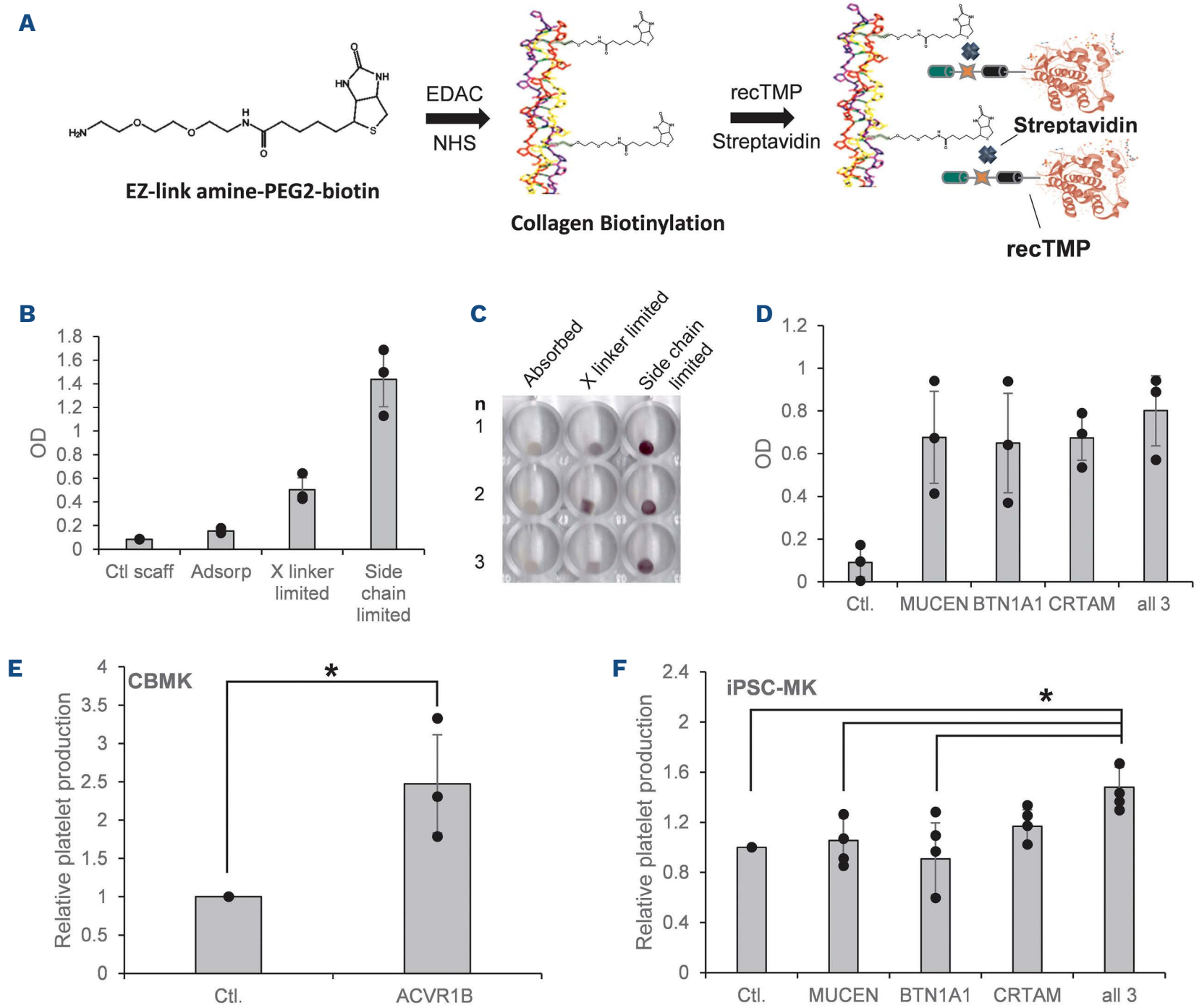


Figure 3. Collagen scaffolds functionalized with recombinant transmembrane proteins increases platelet production. Addition of recombinant transmembrane proteins (recTMP) to modified collagen cell supports via biotin and the multiple binding sites of streptavidin. (A) Scheme for attaching a biotin-tagged recTMP via addition of a biotin to collagen with 1-ethyl-3-(3-dimethylaminopropyl) carbodiimide, hydrochloride/ N-hydroxysuccinimide (EDAC/NHS) crosslinker in the presence of amine-polyethylene glycol (PEG)-biotin (EZ-link), amine provides the moiety to crosslink to collagen with a PEG extender and biotin end, recTMP synthesized with a biotin incorporating sequence can be bound in the presence of streptavidin. (B) Analysis of methods of adsorption, crosslinking with PEG biotin in excess and limiting the concentration of crosslinker (x linker limited), or by adding excess crosslinker and limiting the amount of amine-PEG-biotin (side chain limited), quantified by Cd4 enzyme-linked immunosorbant assay (ELISA), data represents optical density (OD), N=3. (C) 5-bromo-4-chloro-3'-indolylphosphate p-toluidine salt/nitro-blue tetrazolium chloride (BCIP/NBT) dye deposition on collagen support material in triplicate of; adsorbed, crosslinker-limited, or side chain-limited attachment of recTMP. (D) Quantification of candidate recTMP using Cd4 ELISA, data represents optical density, N=3. Quantification of relative platelet production on functionalized collagen scaffolds of (E) cord blood-derived megakaryocytes (CBMK) with 0.01 mg/mL ACVR1B and (F) induced pluripotent stem cell-derived MK (iPSC-MK) with either 0.178 mg/mL MUCEN, 0.355 mg/mL BTN1A1, 0.71 mg/mL CRTAM or all 3 recTMP together, N=4, data compared to streptavidin-only control (Ctl.). All data mean \pm standard deviation, Repeated measures one-way ANOVA with Bonferroni *post hoc*; * $P < 0.05$. scaff: scaffold; Adsorb: adsorption.

Supplementary Figure S7C). The BCIP/NBT analysis of the 3D sponge scaffold showed again even coating of the scaffold when functionalized and protein immobilization was confirmed by ELISA (Online Supplementary Figure S7D, E).

Recombinant transmembrane proteins increase functional platelet production in silk scaffolds

To test the ability of the modified recTMP to support platelet formation we first cultured CBMK and iPSC-MK onto silk films functionalized with the recTMP of interest (Figure 4A). Increased proplatelet formation and branching identified by β 1-tubulin staining of CBMK was observed on silk films functionalized with ACVR1B but not on the control (Figure 4Bi, C), while silk films functionalized with CRTAM, BTN1A1, or MUCEN supported increased production of β 1-tubulin⁺ platelet-like particles by iPSC-MK (Figure 4Bii, D). We finally validated the effect of the recTMP-functionalized 3D sponges using a silk bone marrow model specifically developed for supporting human platelet production

(Figure 5A). 3D reconstruction of functionalized silk scaffolds demonstrated an efficient adhesion and homogeneous distribution of both CBMK or iPSC-MK, as assessed by immunofluorescence confocal microscopy analysis of CFSE-labeled samples (Figure 5B, C). Confocal microscopy imaging of the 3D culture before starting the perfusion also demonstrated the presence of CBMK and iPSC-MK showing the characteristic cytoplasmic rearrangements of proplatelet forming-MK (Figure 5B, C), with the extension of multiple proplatelet shafts. When the culture medium was perfused at $\sim 80 \mu\text{L}/\text{min}$ within the system, the flow allowed the detachment of dumbbell-shaped platelets and disc-shaped platelets of 2–4 μm diameter (Figure 5D, E; Online Supplementary Figure S8). For CBMK, ACVR1B significantly increased platelet production compared to the control (1.5 ± 0.2 , fold change \pm SD; $P < 0.05$; Figure 6F), as assessed by counting CD41⁺CD42b⁺ lineage-specific markers by flow cytometry. For iPSC-MK, functionalized silk scaffolds supported a statistically significant increase in platelet

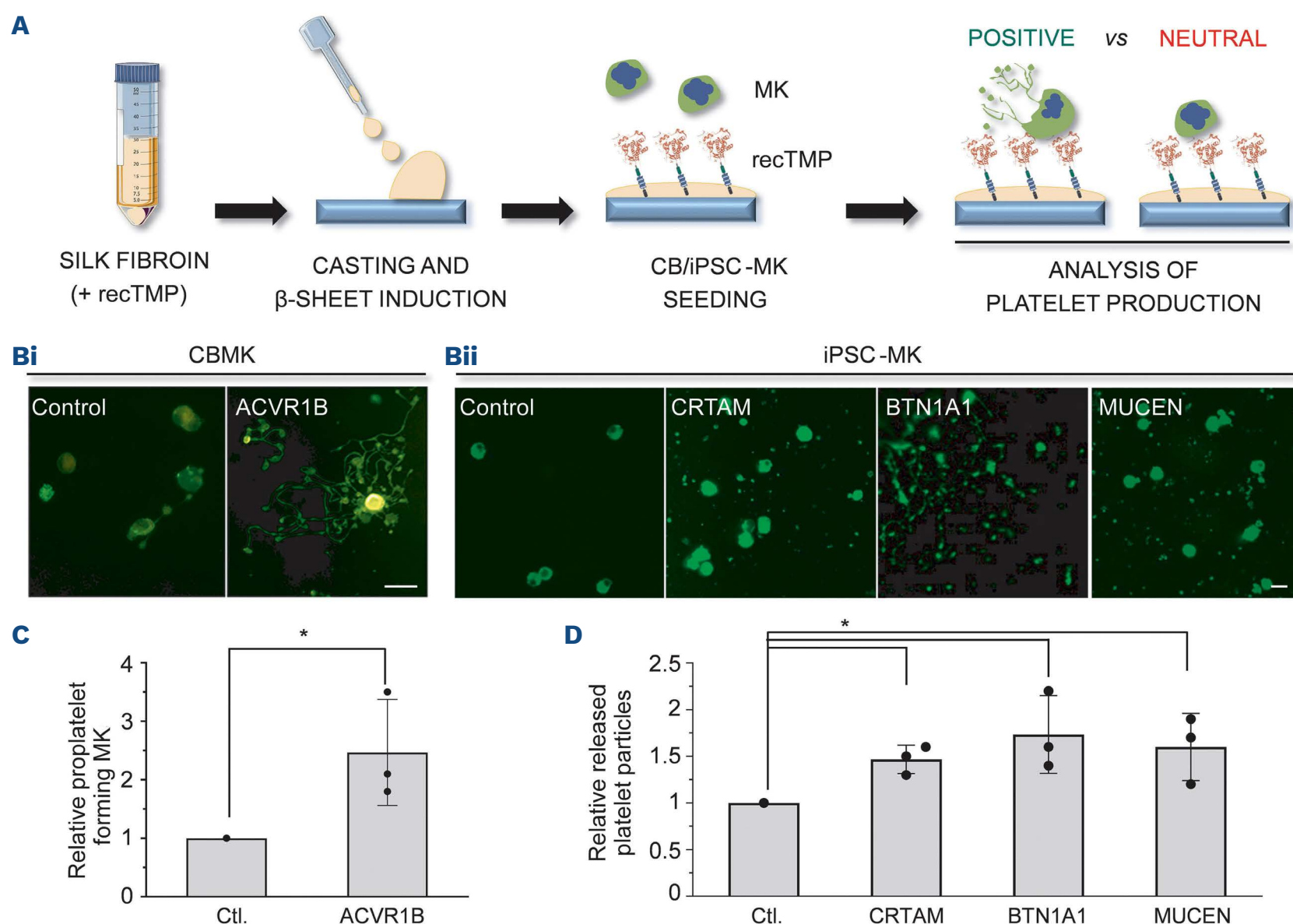


Figure 4. Effect of functionalized silk films on *ex vivo* platelet production. (A) Silk films were prepared by dispensing a silk fibroin solution onto a polydimethylsiloxane (PDMS) mold. When the solution dries, a silk film is formed that contains a dispersion of recombinant transmembrane proteins (recTMP). The film was finally soaked in the culture medium before cell seeding. Representative immunofluorescent images of (Bi) cord blood-derived megakaryocytes (CBMK) and (Bii) induced pluripotent stem cell-derived MK (iPSC-MK) cultures on silk films functionalized with the indicated recTMP (scale bar = 30 μm). (C, D) The positive recTMP supported increased proplatelet formation by CBMK and released platelet particles by iPSC-MK compared to the controls, N=3. All data mean \pm standard deviation, paired student *t* test; * $P < 0.05$. Ctl.: control.

production over the control using either the single recTMP, CRTAM (1.51 ± 0.09), BTN1A1 (1.93 ± 0.2) or MUCEN (2 ± 0.5), or a combination of all 3 (2.5 ± 0.35) (fold change \pm SD; $P<0.05$; Figure 5G). Importantly, the silk scaffolds functionalized with the three peptides demonstrated the production of 2 ± 0.5 iPSC-platelets/MK, signifying a 10 \times increase compared to the other described approaches. Human platelets produced within the silk scaffold have

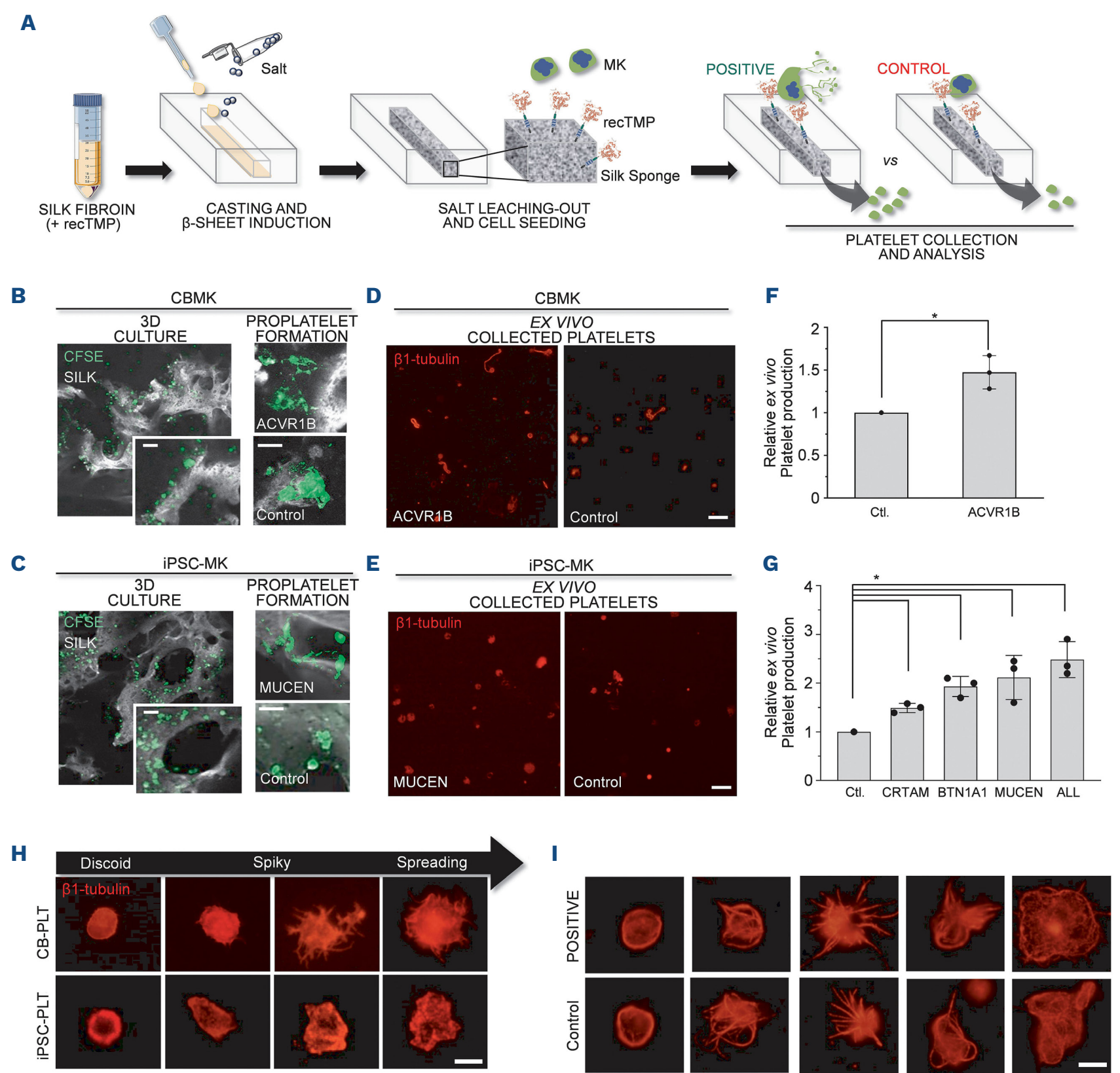


Figure 5. Effect of 3-dimensional silk scaffold functionalization on ex vivo platelet production. (A) The silk sponge was prepared inside a flow chamber by dispensing an aqueous silk solution mixed with salt particles. After leaching out the salt, the resulting porous silk sponge was cultured with cord blood-derived megakaryocytes (CBMK) or induced pluripotent stem cell-derived MK (iPSC-MK) and perfused to allow platelet collection. (B, C) Representative confocal microscopy analysis of CFSE⁺ CBMK and iPSC-MK adhering onto functionalized silk scaffolds upon seeding (green = MK; grey = silk scale bar =100 μ m). After 24-hour incubation into the system the presence of MK elongating proplatelet shafts could be appreciated in the presence of the positive recombinant transmembrane proteins (recTMP), but not of the control (green = MK, grey = silk, scale bars =100 μ m). (D, E) The silk bone marrow was perfused with culture medium for 8 hours and released platelets collected into gas-permeable bags and analyzed by immunofluorescence staining of β 1-tubulin (scale bar =10 μ m). (F, G) Platelet count was assessed by flow cytometry by mixing samples with counting beads and expressed as fold increase relative to the control (N=3). (H, I) β 1-tubulin staining of ex vivo-collected platelets in adhesion on type I collagen over 60 minutes. Platelets were functional as they spread and showed the reorganization of microtubules (scale bars =10 μ m). No difference was observed among control or positive recTMP. All data mean \pm standard deviation, paired student *t* test; **P*<0.05. 3D: 3-dimensional; Ctl.:control.

been demonstrated to share morphological and functional features with peripheral blood platelets.^{24,40}

Ex vivo released platelets from both CBMK and iPSC-MK expressed the characteristic β 1-tubulin coil at their periphery, which was polymerized and re-assembled throughout the platelet cytoplasm upon spreading (Figure 5H). Platelet functionality was not affected by the competent environment whereas spreading of *ex vivo*-collected platelets on collagen type I-coated matrices was comparable between samples from scaffolds functionalized with positive recTMP or the control (Figure 5I).

Discussion

The production of platelets *in vitro* requires the formation of hundreds if not thousands of platelets from each individual MK, matching the efficiency of production *in vivo*. However, in static cultures, the release of *bona fide* live platelets per MK is usually one to one.⁶ Most bioreactors developed to answer this question have sought to recreate physical signals such as shear or turbulence.^{9,10,41} Others have attempted to also recreate chemical signals already known to promote proplatelet formation/platelet release (such as signaling downstream of integrins α IIb β 3) by functionalizing supporting matrices with recombinant proteins, such as fibronectin.^{13,27,42} There is good evidence that cell-to-cell contact between MK and other cell types (particularly endothelial cells) is key to efficient platelet production and this is reproduced in our co-culture data but the proteins involved in this process are largely unknown. In this manuscript we adopt a systematic biology approach whereby we shortlist potential membrane expressed/secreted proteins that may recreate the signaling environment of the platelet-forming niche by mature MK. We subsequently produced a panel of recombinant protein containing the extracellular domain of the candidate proteins together with various tags allowing purification, quantitation and immobilization of these proteins. This allowed us to systematically test several hundred proteins for an effect on platelet production through a direct contact with mature MK. This unbiased approach allowed us to identify novel proteins whose role in platelet formation was unknown. Each of the candidates promoting platelet release identified here had, individually, a small effect size consistent with multiple signaling pathways playing a part within a complex array of “niche signals” that ultimately make platelet production *in vivo* so efficient.

We focused on proteins expressed by only a few cell types here, biased towards endothelial cells. Other cell types have been shown to be key to platelet production such as mesenchymal stromal cells and within the lung vasculature.^{19,43–47} The approach described here could potentially be applied to any cell type likely to promote platelet release, thereby further enriching our understanding of the molecular environment of the niche where MK produced platelets.

In this study, two types of human MK were used: MK differentiated from human cord blood CD34⁺ hematopoietic progenitors and MK differentiated from pluripotent stem cells. Previous reports have shown that, although very similar, both types of MK have their own identity relating to their developmental origin. MK derived from iPSC show a more “embryonic” identity whilst CBMK are closer to adult MK resulting from “definitive” hematopoiesis.^{14,48,49} Both types of MK release their platelets in different niches, the embryonic MK in the yolk sac and fetal liver, whilst the CBMK release their platelet in the bone marrow and fully mature vascular circulation. We show in this study that these differences are reflected in the proteins that promote platelet release by these two types of MK with some promoting platelet release in both types of MK whilst others were specifically targeting one or the other type of MK.

The production of cellular therapies *in vitro* is rapidly expanding, particularly following the discovery of iPSC. However, one of the main limitations of the technology is obtaining a pure product and clinically relevant yield at affordable cost.^{50,51} The 3D collagen and silk scaffolds used here have been previously shown to yield functional platelet harvest. We show here how the design of different tags added to the recTMP allowed us to functionalize both types of scaffolds. More importantly we show a 3-fold gain in platelet production in the silk scaffold whilst retaining platelet functionality. This would have a significant impact on the manufacturing costs by reducing the volume of MK culture 3-fold and therefore the production costs which are mostly driven by the cytokines used in the liquid MK cultures.⁵¹ Lawrence *et al.* uses a costing model for GMP production of platelets in 2-dimensional static systems (no automation). This predicts the costing of one *in vitro*-derived platelet unit as £149,571 as opposed to a donor-derived platelet unit costing £271.21 (2024/25).^{51,52} Although it is important to note that NHS costings are underestimated as they do not include all costs such as staff time, storage, laboratory testing.⁵³ The production of recombinant proteins to functionalize the scaffold is of course not insignificant. Identification of the pathways the recTMP stimulate in the MK may pinpoint druggable targets, allowing us to use small molecule rather than full length proteins to reproduce the effect on platelet production.

The potential application of the technologies described here goes well beyond the production of platelets *in vitro*. The concept of *in vivo* niche reproduction *in vitro* to promote cellular differentiation is not new, exemplified by the multiple applications of 3D scaffolds to promote cellular production/regeneration with a wide array of cell types and by the emergence of the field of “organoids”.^{54–59} Organoids are organized 3D cell collection, particularly containing different cell types that positively promote each other’s growth, maturity and functionality. Our approach would allow to potentially dissect these cell-to-cell interactions and potentially lead to major gain towards larger scale production of cell types *in vitro* for clinical applications.

Disclosures

No conflicts of interests to disclose.

Contributions

Conceptualization by HRF, MC, GB and CG. Methodology by HRF, MC, GB, YY, NMS, GJW, DH, CADB, AB, MEP, PBM, TM, ALE, ND, JHS, SMB, REC and ET. Investigation by HRF, MC, GB, YY, NMS, GJW, DH, CADB, AB, MEP, PBM, AKW, WAS, ND, JHS, SMB and ET. Visualization by HRF, MC, GB, YY, NMS, GJW, DH, CADB, AB, ET and CG. Supervision by CG, AB and GJW. Writing of the original draft by HRF, MC, GB, YY, NMS, GJW, DH, CADB, AB, MEP, PBM, ET and CG. Manuscript reviewing and editing by CADB, AB, CG and HRF.

Acknowledgments

The authors thank the Cambridge Blood and Stem Cell Biobank for providing the cord blood used in this study.

Funding

The study was funded by NHS Blood and Transplant (WP15-06) (to HRF and MA), the Medical Research Council Center (MR/L022982/1) (to GB), the National Institute for Health Research (NIHR; RP-PG-0310-1002) (to MC), the Wellcome Trust (206194), the Science Foundation Ireland (19/FIP/AI/7490) (to PBM), EU Horizon 2020 (767309) (to DH and AKW), the European Research Council (ERC) (320598 3D-E) (to SMB and REC), NHS Blood and Transplant (to CG), the European Commission grant (H2020-FETOPEN-1-2016-2017-SilkFusion, grant agreement 767309) (to AB and CG), the US National Institutes of Health (R01 EB016041-02) (to AB and CG).

Data-sharing statement

For original data please contact CG. Additional methods used in this study are included in the Online Supplementary Appendix.

References

- Cowan K. Strategies to reduce inappropriate use of platelet transfusions. *Nursing Times* [online] 2017;113(2):18-21.
- Moreau T, Evans AL, Vasquez L, et al. Large-scale production of megakaryocytes from human pluripotent stem cells by chemically defined forward programming. *Nat Commun*. 2016;7:11208.
- Feng Q, Shabrani N, Thon JN, et al. Scalable generation of universal platelets from human induced pluripotent stem cells. *Stem Cell Rep*. 2014;3(5):817-831.
- Nakamura S, Takayama N, Hirata S, et al. Expandable megakaryocyte cell lines enable clinically applicable generation of platelets from human induced pluripotent stem cells. *Cell Stem Cell*. 2014;14(4):535-548.
- Suzuki D, Flahou C, Yoshikawa N, et al. iPSC-derived platelets depleted of HLA class I are inert to anti-HLA class I and natural killer cell immunity. *Stem Cell Rep*. 2020;14(1):49-59.
- Shepherd J, Howard D, Waller A, et al. Structurally graduated collagen scaffolds applied to the ex vivo generation of platelets from human pluripotent stem cell-derived megakaryocytes: enhancing production and purity. *Biomaterials*. 2018;182:135-144.
- Junt T, Schulze H, Chen Z, et al. Dynamic visualization of thrombopoiesis within bone marrow. *Science*. 2007;317(5845):1767-1770.
- Thon JN, Dykstra BJ, Beaulieu LM. Platelet bioreactor: accelerated evolution of design and manufacture. *Platelets*. 2017;28(5):472-477.
- Blin A, Le Goff A, Magniez A, et al. Microfluidic model of the platelet-generating organ: beyond bone marrow biomimetics. *Sci Rep*. 2016;6:21700.
- Ito Y, Nakamura S, Sugimoto N, et al. Turbulence activates platelet biogenesis to enable clinical scale ex vivo production. *Cell*. 2018;174(3):636-648.e18.
- Nakagawa Y, Nakamura S, Nakajima M, et al. Two differential flows in a bioreactor promoted platelet generation from human pluripotent stem cell-derived megakaryocytes. *Exp Hematol*. 2013;41(8):742-748.
- Avanzi MP, Oluwadara OE, Cushing MM, Mitchell ML, Fischer S, Mitchell WB. A novel bioreactor and culture method drives high yields of platelets from stem cells. *Transfusion*. 2016;56(1):170-178.
- Dunois-Larde C, Capron C, Fichelson S, Bauer T, Cramer-Borde E, Baruch D. Exposure of human megakaryocytes to high shear rates accelerates platelet production. *Blood*. 2009;114(9):1875-1883.
- Evans AL, Dalby A, Foster HR, et al. Transfer to the clinic: refining forward programming of hPSCs to megakaryocytes for platelet production in bioreactors. *Blood Adv*. 2021;5(7):1977-1990.
- Rafii S, Shapiro F, Pettengell R, et al. Human bone-marrow microvascular endothelial-cells support long-term proliferation and differentiation of myeloid and megakaryocytic progenitors. *Blood*. 1995;86(9):3353-3363.
- Avecilla ST, Hattori K, Heissig B, et al. Chemokine-mediated interaction of hematopoietic progenitors with the bone marrow vascular niche is required for thrombopoiesis. *Nat Med*. 2004;10(1):64-71.
- Hamada T, Mohle R, Hesselgesser J, et al. Transendothelial migration of megakaryocytes in response to stromal cell-derived factor 1 (SDF-1) enhances platelet formation. *J Exp Med*. 1998;188(3):539-548.
- Pitchford SC, Lodie T, Rankin SM. VEGFR1 stimulates a CXCR4-dependent translocation of megakaryocytes to the vascular niche, enhancing platelet production in mice. *Blood*. 2012;120(14):2787-2795.
- Mendelson A, Strat AN, Bao WL, et al. Mesenchymal stromal cells lower platelet activation and assist in platelet formation in vitro. *JCI Insight*. 2019;4(16):e126982.
- Sun Y, Vandenbrielle C, Kauskot A, Verhamme P, Hoylaerts MF, Wright GJ. PEAR1: a novel link between ige-mediated allergy and cardiovascular disease. *J Thromb Haemost*. 2015;13:256-256.
- Machlus KR, Johnson KE, Kulenthirarajan R, et al. CCL5 derived from platelets increases megakaryocyte proplatelet formation. *Blood*. 2016;127(7):921-926.
- Di Buduo CA, Soprano PM, Miguel CP, Perotti C, Del Fante C, Balduini A. A gold standard protocol for human megakaryocyte culture based on the analysis of 1,500 umbilical cord blood samples. *Thromb Haemost*. 2021;121(4):538-542.
- Bariana TK, Labarque V, Heremans J, et al. Sphingolipid dysregulation due to lack of functional KDSR impairs proplatelet formation causing thrombocytopenia. *Haematologica*. 2019;104(5):1036-1045.
- Di Buduo CA, Soprano PM, Tozzi L, et al. Modular flow chamber for engineering bone marrow architecture and function. *Biomaterials*.

- 2017;146:60–71.
25. Ashworth JC, Mehr M, Buxton PG, Best SM, Cameron RE. Parameterizing the transport pathways for cell invasion in complex scaffold architectures. *Tissue Eng Part C Methods*. 2016;22(5):409–417.
 26. Davidenko N, Schuster CF, Bax DV, et al. Control of crosslinking for tailoring collagen-based scaffolds stability and mechanics. *Acta Biomater*. 2015;25:131–142.
 27. Abbonante V, Di Buduo CA, Gruppi C, et al. A new path to platelet production through matrix sensing. *Haematologica*. 2017;102(7):1150–1160.
 28. Eto K, Murphy R, Kerrigan SW, et al. Megakaryocytes derived from embryonic stem cells implicate CalDAG-GEFI in integrin signaling. *Proc Natl Acad Sci U S A*. 2002;99(20):12819–12824.
 29. Gaur M, Kamata T, Wang S, Moran B, Shattil SJ, Leavitt AD. Megakaryocytes derived from human embryonic stem cells: a genetically tractable system to study megakaryocytopoiesis and integrin function. *J Thromb Haemost*. 2006;4(2):436–442.
 30. Kotha S, Sun SJ, Adams A, et al. Microvasculature-directed thrombopoiesis in a 3D *in vitro* marrow microenvironment. *PLoS One*. 2018;13(4):e0195082.
 31. Cheng LZ, Qasba P, Vanguri P, Thiede MA. Human mesenchymal stem cells support megakaryocyte and pro-platelet formation from CD34(+) hematopoietic progenitor cells. *J Cell Physiol*. 2000;184(1):58–69.
 32. Majumdar MK, Keane-Moore M, Buyaner D, et al. Characterization and functionality of cell surface molecules on human mesenchymal stem cells. *J Biomed Sci*. 2003;10(2):228–241.
 33. Angelopoulou M, Novelli E, Grove JE, et al. Cotransplantation of human mesenchymal stem cells enhances human myelopoiesis and megakaryocytopoiesis in NOD/SCID mice. *Exp Hematol*. 2003;31(5):413–420.
 34. Xiao M, Wang YK, Tao C, et al. Osteoblasts support megakaryopoiesis through production of interleukin-9. *Blood*. 2017;129(24):3196–3209.
 35. Pallotta I, Lovett M, Rice W, Kaplan DL, Balduini A. Bone marrow osteoblastic niche: a new model to study physiological regulation of megakaryopoiesis. *PLoS One*. 2009;4(12):e8359.
 36. D'Atri LP, Pozner RG, Nahmod KA, et al. Paracrine regulation of megakaryo/thrombopoiesis by macrophages. *Exp Hematol*. 2011;39(7):763–772.
 37. Tijssen MR, Cvejic A, Joshi A, et al. Genome-wide analysis of simultaneous GATA1/2, RUNX1, FLI1, and SCL binding in megakaryocytes identifies hematopoietic regulators. *Develop Cell*. 2011;20(5):597–609.
 38. Sun Y, Vandenbriele C, Kauskot A, Verhamme P, Hoylaerts MF, Wright GJ. A Human platelet receptor protein microarray identifies the high affinity immunoglobulin E receptor subunit α (Fc ϵ R1 α) as an activating platelet endothelium aggregation receptor 1 (PEAR1) ligand. *Mol Cell Proteomics*. 2015;14(5):1265–1274.
 39. An B, DesRochers TM, Qin G, et al. The influence of specific binding of collagen-silk chimeras to silk biomaterials on hMSC behavior. *Biomaterials*. 2013;34(2):402–412.
 40. Di Buduo CA, Wray LS, Tozzi L, et al. Programmable 3D silk bone marrow niche for platelet generation *ex vivo* and modeling of megakaryopoiesis pathologies. *Blood*. 2015;125(14):2254–2264.
 41. Thon JN, Mazutis L, Wu S, et al. Platelet bioreactor-on-a-chip. *Blood*. 2014;124(12):1857–1867.
 42. Tozzi L, Laurent PA, Di Buduo CA, et al. Multi-channel silk sponge mimicking bone marrow vascular niche for platelet production. *Biomaterials*. 2018;178:122–133.
 43. Lefrançois E, Ortiz-Muñoz G, Caudrillier A, et al. The lung is a site of platelet biogenesis and a reservoir for haematopoietic progenitors. *Nature*. 2017;544(7648):105–109.
 44. Pariser D, Hilt Z, Ture S, et al. Lung megakaryocytes are immune modulatory cells. *J Clin Invest*. 2021;131(1):e137377.
 45. Livada A, Mcgrath K, Malloy M, et al. Long-lived lung megakaryocytes contribute to platelet recovery in thrombocytopenia models. *J Clin Invest*. 2024;134(22):181111.
 46. Kaufman R, Airo R, Pollack S, Crosby W. Circulating megakaryocytes and platelet release in lung. *Blood*. 1965;26(6):720.
 47. Howell W, Donahue D. The production of blood platelets in the lungs. *J Exp Med*. 1937;65(2):177–203.
 48. Bluteau O, Langlois T, Rivera-Munoz P, et al. Developmental changes in human megakaryopoiesis. *J Thromb Haemost*. 2013;11(9):1730–1741.
 49. Kammers K, Taub MA, Mathias RA, et al. Gene and protein expression in human megakaryocytes derived from induced pluripotent stem cells. *J Thromb Haemost*. 2021;19(7):1783–1799.
 50. Di Buduo CA, Aguilar A, Soprano PM, et al. Latest culture techniques: cracking the secrets of bone marrow to mass-produce erythrocytes and platelets. *Haematologica*. 2021;106(4):947–957.
 51. Lawrence M, Evans A, Moreau T, et al. Process analysis of pluripotent stem cell differentiation to megakaryocytes to make platelets applying European GMP. *NPJ Regen Med*. 2021;6(1):27.
 52. NHS Blood and Transplant. Price list 2024–2025. <https://hospital.blood.co.uk/components/portfolio-and-prices/>. Accessed January 2025.
 53. Agrawal S, Davidson N, Walker M, et al. Assessing the total costs of blood delivery to hospital oncology and haematology patients. *Curr Med Res Opin*. 2006;22(10):1903–1909.
 54. Zhu MF, Li W, Dong XH, et al. *In vivo* engineered extracellular matrix scaffolds with instructive niches for oriented tissue regeneration. *Nat Commun*. 2019;10(1):4620.
 55. Bassi G, Panseri S, Dozio SM, et al. Scaffold-based 3D cellular models mimicking the heterogeneity of osteosarcoma stem cell niche. *Sci Rep*. 2020;10(1):4620.
 56. Congrains A, Bianco J, Rosa RG, Mancuso RI, Saad STO. 3D scaffolds to model the hematopoietic stem cell niche: applications and perspectives. *Materials (Basel)*. 2021;14(3):569.
 57. Colzani M, Malcor JD, Hunter EJ, et al. Modulating hESC-derived cardiomyocyte and endothelial cell function with triple-helical peptides for heart tissue engineering. *Biomaterials*. 2021;269:120612.
 58. Creff J, Courson R, Mangeat T, et al. Fabrication of 3D scaffolds reproducing intestinal epithelium topography by high-resolution 3D stereolithography. *Biomaterials*. 2019;221:119404.
 59. Hofer M, Lutolf MP. Engineering organoids. *Nat Rev Mater*. 2021;6(5):402–420.